NASA TECHNICAL NOTE

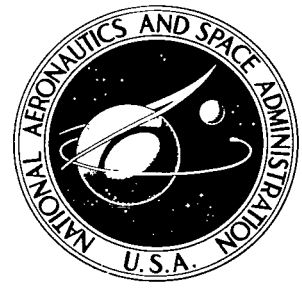

NASA TN D-5624
c. 1

NASA TN D-5624

THERMOCAPILLARY INDUCED BREAKDOWN OF A FALLING LIQUID FILM

by Frederick F. Simon and Yih-Yun Hsu

Lewis Research Center
Cleveland, Ohio

NATIONAL AERONAUTICS AND SPACE ADMINISTRATION • WASHINGTON, D. C. • JANUARY 1970

1. Report No. NASA TN D-5624	2. Government Accession No.	3. Recipient's Catalog No.
4. Title and Subtitle THERMOCAPILLARY INDUCED BREAKDOWN OF A FALLING LIQUID FILM		5. Report Date January 1970 6. Performing Organization Code
7. Author(s) Frederick F. Simon and Yih-Yun Hsu		8. Performing Organization Report No. E-4520
9. Performing Organization Name and Address Lewis Research Center National Aeronautics and Space Administration Cleveland, Ohio 44135		10. Work Unit No. 120-01 11. Contract or Grant No.
12. Sponsoring Agency Name and Address National Aeronautics and Space Administration Washington, D.C. 20546		13. Type of Report and Period Covered Technical Note 14. Sponsoring Agency Code

15. Supplementary Notes

16. Abstract

A study was made of the breakdown due to heating of a falling liquid film. Heating is believed to create thermocapillary effects which cause the film breakdown. Visual observation of the formation of a critical film thickness prior to film breakdown was used to formulate an analytical equation for correlating the experimental data.

17. Key Words (Suggested by Author(s)) Film stability Heating Thermocapillary Falling film Waves	18. Distribution Statement Unclassified - unlimited	
19. Security Classif. (of this report) Unclassified	20. Security Classif. (of this page) Unclassified	21. No. of Pages 35
		22. Price* $3.00

*For sale by the Clearinghouse for Federal Scientific and Technical Information
Springfield, Virginia 22151

THERMOCAPILLARY INDUCED BREAKDOWN OF A FALLING LIQUID FILM

by Frederick F. Simon and Yih-Yun Hsu

Lewis Research Center

SUMMARY

An experimental and analytical investigation was made of the breakdown due to heating of a falling subcooled liquid film (distilled water and glycerol-water solution). Heating of a liquid film is believed to create lateral surface tension gradients which cause film breakdown. The mechanism by which the breakdown occurs was studied, and the results were used as a basis for an analytical model. The analytical results were correlated with experimental film breakdown data.

Two regions of film breakdown were found. One region, called the capillary-wave region, behaved according to an analysis. The analysis predicts that the product of breakdown heat flux and heating length is a function of fluid properties (including temperature coefficient of surface tension), and the logarithm of the ratio of the initial film thickness to the minimum film thickness. The other region (roll wave) occurs at a higher flow rate, and the data plot according to the fluid used. In this region film breakdown oscillates between a dry and a wetted surface condition. The film thickness that marks the transition from one region to another was predictable according to an analysis using a balance of momentum and surface forces.

INTRODUCTION

The stability of a moving liquid film is an important consideration when such a film is being used to cool a heated surface. The annular flow regime of two-phase flow in a channel is an example of a moving liquid film which must remain stable to permit controlled performance of the heating surface. A breakdown of the liquid film could result in overheating of the exposed surface.

One cause of film breakdown is the disruptive action of surface-tension gradients at the free surface of a liquid film. If the shear force due to surface tension variation is high compared with hydrodynamic forces, it will be possible for surface motion and

eventually bulk motion to occur. This motion can lead to film breakdown. In this report, breakdown of a heated falling film is studied mainly from the point of view that the breakdown occurs as a result of temperature dependent surface tension variation (thermocapillary effect). Other possible mechanisms causing film breakdown include evaporation, ebullition, and the variation of viscosity with temperature. Ebullition is a competitive process and prevails when the film temperature is high and the film thickness is thick, as was discussed in reference 1. The other two mechanisms are considered unimportant for the present study. (See appendixes A and B.)

The motion that can occur in a thin liquid film as a result of surface tension variation was discussed and analyzed by Levich (ref. 2). He considers the case of surface tension variation due to temperature effects and concentration effects. Yih (ref. 3) analyzed the motion caused by the surface tension variation resulting from concentration effects. By the use of heated point source to provide a temperature gradient at the free surface of a liquid film, Mitchell and Quinn (ref. 4) observed what they consider to be surface motion caused by surface tension gradients. The motion set up by surface tension variations can, in some instances, be unstable. The analytical results of Yih (ref. 5) show surface tension gradients as a destabilizing influence on laminar parallel flow causing unstable wave motion. In the case of a vertical liquid film, unstable wave motion caused by thermocapillary effects was analyzed by Ludviksson and Lightfoot (ref. 6). Stability analyses (refs. 7 to 10) have shown that surface-tension variation has a strong role in Benard cell instability. These analytical studies confirm the experimental results of Block (ref. 11) who demonstrated that Benard cells in thin films were governed by surface-tension gradients. In some experimental works surface-tension variation has been the reason given for the breakdown of a liquid film. Surface-tension variation was believed to be the cause of the breakdown of a vertical liquid film in an absorption column (ref. 12) and in the heating of a liquid film (refs. 1, 13, and 14). In reference 1, the thermocapillary instability of a falling film was studied. It was found that thermocapillary instability could occur only in thin films without strong turbulence and that a developing length, of the order of 1 centimeter, was needed for the thermal fluctuation to penetrate the film to the interface. It was also found that the ebullition process was a mechanism competing with the thermocapillary force as a source of disturbance for heated film flow. These two mechanisms appear to be mutually exclusive.

Thermal fluctuation at the interface could be due to a nonuniform heat flux, or it could be due to nonuniformity of the film thickness. The film thickness nonuniformity is most probably due to the presence of waves, which has been the subject of many studies. Analyses for the inception of waves in a falling film have been made by Shibuya (ref. 15), Yih (ref. 16), Kapitsa (ref. 17), Benjamin (ref. 18), and others. However, in this report we are more concerned about the role the waves play in the breakdown of a liquid film. The presence of waves is considered to be one cause of introducing fluctuations in

the film thickness. An analysis by Kapitsa (ref. 2) for the wavy structure of film flow is useful.

For this investigation a visual study was made for a falling film outside a metal tube to provide a better understanding of the mechanism of film breakdown. The information allowed the formulation of a hydrodynamic model for analytical purposes. The heat flux required to break down a falling liquid film is then determined experimentally for fluids flowing down inside a glass tube. The fluids studied were distilled water and a glycerol-water solution (45 percent glycerol by wt.). The heating length is varied as a means of checking the significance given to this variable in reference 1. The experimental data are then compared with the analysis.

SYMBOLS

A	parameter defined in eq. (A21)
b	integration constant
c	circumference of ring, cm
F	force, N
f_c	correction factor from ref. 22
g	acceleration of gravity, 9.8 m/sec
h	average film thickness, m
h^+	dimensionless film thickness, y^+ at film surface
i	heat of vaporization, j/kg
k	thermal conductivity, W/(m)(K)
L	length, m
q	heat flux, W/m^2
T	temperature, K
t	thickness of glass, m
U	x-component of velocity, m/sec
U^*	characteristic velocity, $\sqrt{\tau_0/\rho}$, m/sec
U^+	dimensionless velocity, U/U^*
W	z-component of velocity, m/sec

We	Weber number, dimensionless
x	distance along heating surface in flow direction
y	perpendicular distance from heating surface
y^+	dimensionless distance, $yU^*\rho/\mu$
z	coordinate perpendicular to x and y
β	property grouping, $\gamma/\rho k$
Γ	mass flow rate, kg/(m)(sec)
γ	temperature coefficient of surface tension, N/(m)(K)
λ	wavelength, m
μ	viscosity, N-sec/m^2
ρ	density, kg/m^3
σ	surface tension, N/m
τ_0	shear stress at wall in x-direction, N/m^2
φ	contact angle

Subscripts:

B	breakdown condition
f	final
g	glass
h	liquid-gas interface
i	inside
min	minimum
o	outside
p	peak film thickness in wavy flow
w	wall
0	initial condition

Supercripts:

—	average
*	wetting condition

VISUAL STUDY OF THE HYDRODYNAMICS OF FILM BREAKDOWN

An understanding of the hydrodynamics of film breakdown is an important aid to the analysis of liquid film breakdown. Such information is needed for establishing a film model to be analyzed. To investigate the hydrodynamics of film breakdown, a visual experiment was performed. A glycerol-water mixture (45 percent glycerol by wt.) and water were caused to flow over the outside surface of a 0.9-meter long, 1.3-centimeter-diameter Inconel tube. An electrical heater was placed inside the Inconel tube. Heat was applied to the tube in steps, and at each power level the film flow was observed and photographed. Photographs of the glycerol-water mixture for some of the power levels are shown in figure 1. The appearance of surface waves in figure 1 was accentuated by having the lighting and the camera at an angle of approximately 45° with the axis of the vertical tube. The amplitude of the waves is higher for a thicker film. Consequently, the wave image is more pronounced for a thicker film. This makes it possible for the surface waves to act as an index to what is happening to the falling liquid film as a result of the heating. The visual experiment was begun at the no heat condition (fig. 1(a)). With application of power to the Inconel tube, a redistribution of the liquid flow was noted. This redistribution occured gradually along the heated length of the tube. The result was an eccentric distribution of the liquid flow around the tube with one side of the tube having a thinning liquid film. An example of such redistribution is shown in figure 1(b). A further increase in the heating rate causes a greater thinning of the liquid film. A heating condition is finally reached where the liquid film thins down so much that it is unstable and quickly breaks down causing a dry area to form. This may be seen in figure 1(c). To make the formation of a dry area more distinct, a thin coating of china clay was put on the tube and a series of photographic runs made with water flowing outside the tube. The thinning of the liquid film is evident in the three photographs of figure 2. The explanation for this thinning is the same as that for the glycerol-water runs. The formation of a dry wall condition (fig. 2(c)) is made more evident by the whitening of the china clay when it becomes dry. The sequence of pictures in figures 1 and 2 indicates the existence of a secondary motion. This secondary motion has a circumferential path which begins at the side of the tube that finally shows a dry area. It was observed that the film thins down to a finite thickness and then quickly breaks down instead of thinning down in a continuous manner to a zero film thickness. It is assumed, that when breakdown occurs, the minimum film thickness is the same as that in the adiabatic case. In other words, we assume that for a given fluid-surface combination there exists a minimum film thickness below which the film can be broken down because of any small perturbation. The breakdown occurs as soon as the minimum thickness is reached but is independent of the process through which this film thickness is reached. In this report

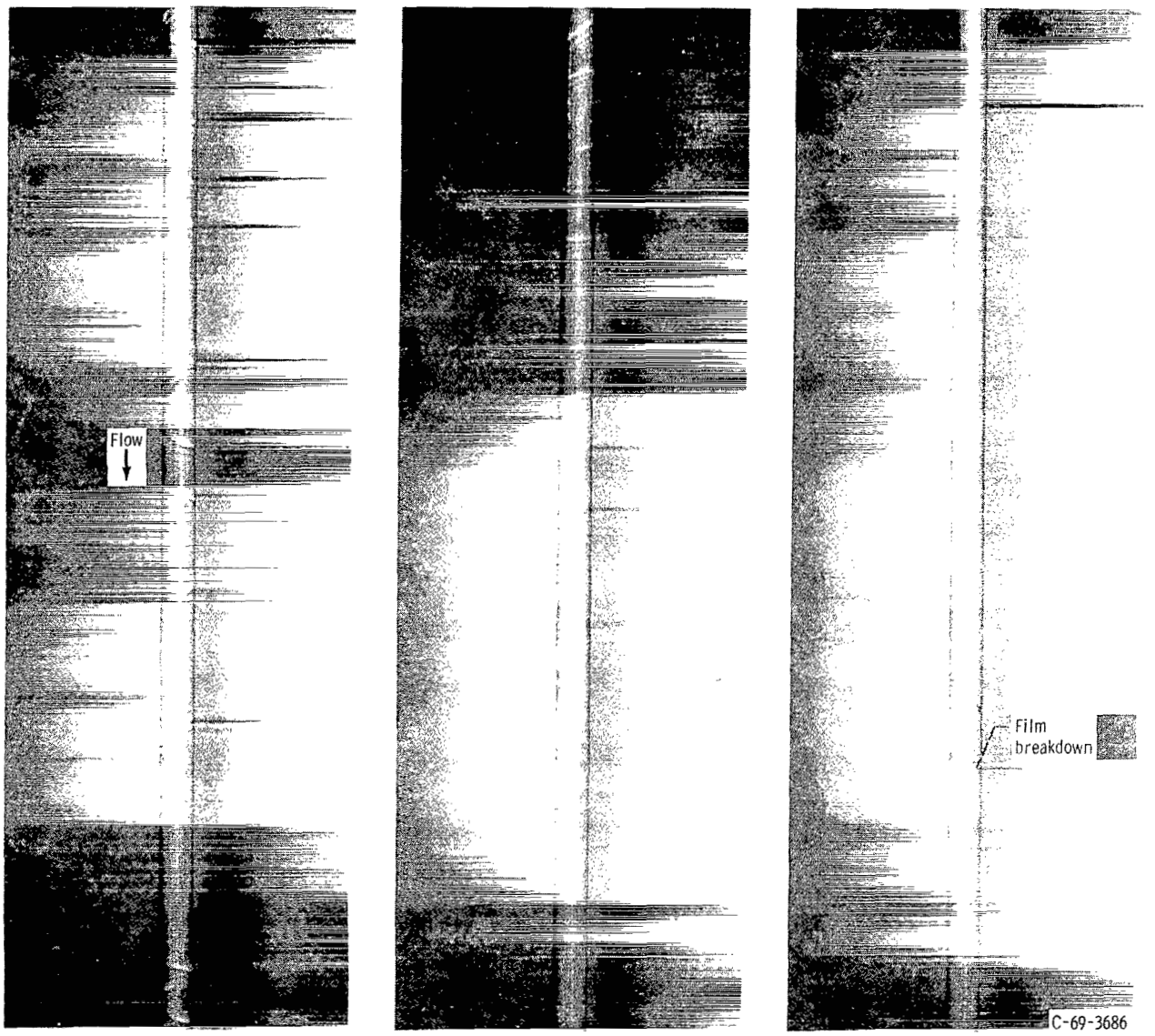

(a) Zero heat flux. (b) Increasing heat flux. (c) Film breakdown heat flux.

Figure 1. - Visual evidence of film breakdown (glycerol - water).

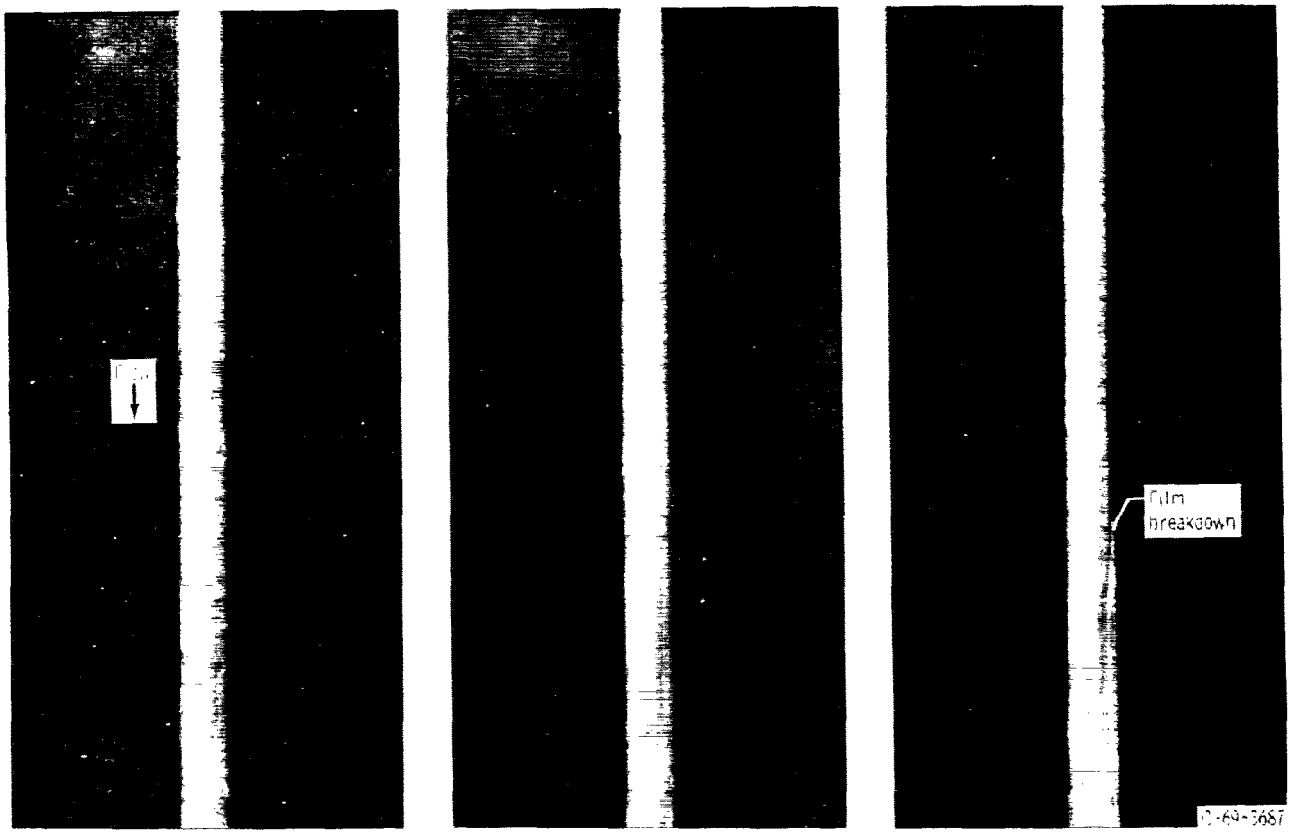

(a) Zero heat flux. (b) Increasing heat flux. (c) Film breakdown heat flux.

Figure 2. - Visual evidence of film breakdown (water).

we are concerned with how thermocapillary effects cause a minimum film thickness condition to occur.

ANALYSIS - POSTULATION OF MODEL

For the purpose of analysis, the visual results of the previous section are translated into a flat plate model (fig. 3). For the ratio of film thickness to tube diameter involved in this study, such an assumption is valid. Figure 3(a) shows the streamlines that occur as result of thermocapillary driven secondary motion. The film thickness noted at the initial position ($h = h_0$) would remain a constant over the entire surface if there were no thermal effects to disturb the film. As a result of heat transfer, the liquid streamlines are altered and the film thickness is reduced to a minimum wetting value ($h = h_{min}$). When the conditions are reached for the minimum wetting thickness to occur, the film breaks down and, a dry area appears. Assuming the thermal effect to be chiefly a thermocapillary one, a section of the main flow is shown in figure 3(b) with the shear

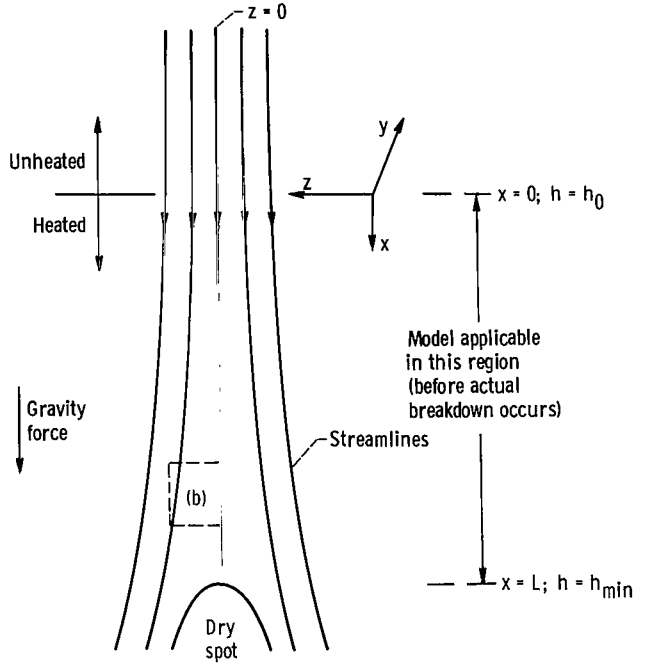

(a) Model of flow distribution due to thermocapillary effects and resulting dry spot formation.

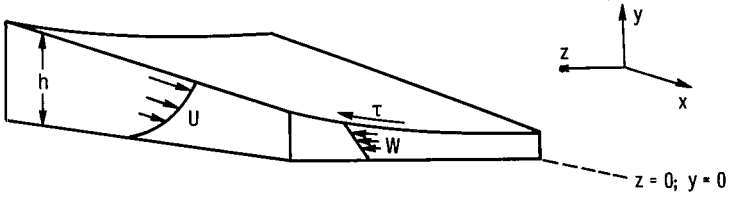

(b) Section of liquid film showing crossflow created by thermocapillary action.

Figure 3. - Film breakdown model.

stress due to thermocapillary force. Also shown in figure 3(b) is the main flow in the vertical x direction and the secondary flow in the horizontal direction. The secondary flow is a result of the surface tangential shear caused by thermocapillary forces. Surface forces will occur in the directions other than the z-direction; however, the z-direction force is assumed to be the most effective force in producing the secondary flow. A surface force in the x-direction cannot have much effect because of the dominating influence of the gravitational force.

Appendix C presents an analysis of the liquid motion caused by lateral surface tension gradients, which results in the liquid film being reduced to a minimum stable value ($h = h_{min}$). It should be emphasized that the analysis applies prior to, but not after, the physical breakdown of the film. With equations (C1) to (C5) and the boundary conditions that $U = W = 0$ at $y = 0$ and $W = (d\sigma/dT)(\partial T/\partial z)(h/\mu)$ at $y = h$, and the fact that the film breaks down at $h = h_{min}$, one can obtain (as shown in appendix C) the solution for the thinning and eventual breakdown of the film as

$$\frac{h_{min}}{h_0} = \exp\left[\frac{2\gamma q_{w,B} b^2 (L - x_0)}{g\rho k}\right] \tag{C30}$$

or

$$q_{w,B} = \frac{g\rho k}{(L - x_0)2\gamma b^2} \ln \frac{h_{min}}{h_0} \tag{C31}$$

In this equation all the terms on the right hand side can be determined except the parameter b^2. Assuming b^2 to be a constant for all fluids, equation (B31) serves as a functional relation between the basic variables and thus can be tried in the correlation of the experimental data. The physical meaning of b^2 will be discussed later.

APPARATUS AND PROCEDURE

Apparatus

A basic requirement in the experimental determination of liquid film breakdown inside a tube is to visually observe a falling film which is being heated. This was accomplished by electrical heating of a conducting glass tube (11-mm i. d.) in which there was internal flow of liquid. The thin electrically conducting surface on the outside of the

glass tube permitted resistance heating of the tube without interfering with visualizations of the liquid annular film. Power to the tube was measured by a voltmeter, an ammeter, and a wattmeter. The conducting glass tube is shown schematically along with the auxiliary apparatus in figure 4. Three heating lengths were used as noted in the figure. An unheated entrance length of 0.39 meter was provided to permit a fully developed liquid film. The system was set up to maintain cleanliness of the fluid being studied. This was necessary to prevent, as much as possible, contamination from affecting the surface tension of the liquid. A pinch pump made it possible for liquid to be

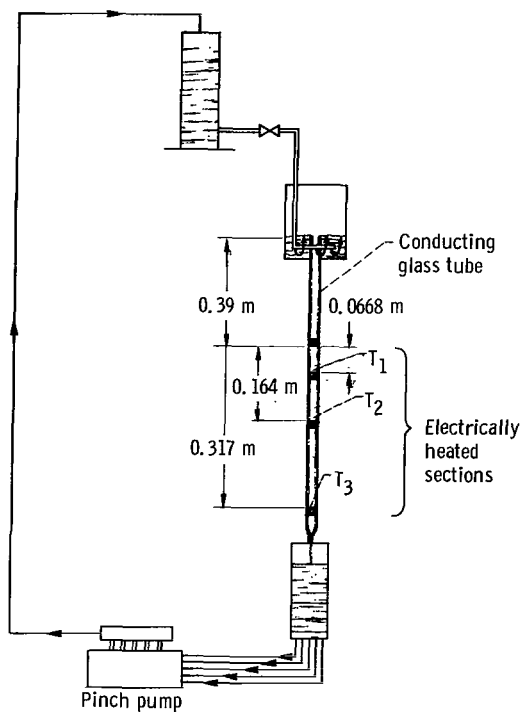

Figure 4. - Experimental apparatus.

circulated without it making contact with possible contaminants such as lubricants or gasket compounds. Liquid within the tubing was squeezed by the pinch pump to a reservoir above the conducting glass tube. The reservoir was used as a means of producing flow without the oscillation caused by the pinch pump. The flow could be controlled by having a valve at the exit of the reservoir.

Film Flow Rate and Film Thickness

Uniformity of the liquid film within the glass tube was believed to occur when a symmetrical pattern of liquid formed at the tube outlet. Flow rates were determined by using a stop watch to time a volume of the liquid collected in a graduate cylinder downstream of the test section. Bulk temperatures were measured in a cylinder at the exit of the tube. Liquid flow rate and bulk temperatures permitted calculation of the initial film thickness according to Nusselt's (ref. 19) equation:

$$h_0 = \left(\frac{3\Gamma\mu}{\rho^2 g}\right)^{1/3} \tag{1}$$

Breakdown Heat Flux

Once the liquid flow was adjusted, electrical power was applied to the conducting glass tube. Electrical power was increased in small increments. At each increment of power an observation was made of the liquid film, and a recording was made of the power, outside wall temperature, bulk temperature, and observations. Use of the power measurement and the outside wall temperature permitted calculation of the inside wall temperature by using the following conduction equation:

$$T_{wi} = T_{wo} - \frac{qt}{k_g} \tag{2a}$$

As the liquid film approached the breakdown point an oscillation of the wall temperature near the end of the heating length was noted. A few increments of power beyond this condition film breakdown occurred. Because of the difficulty in observing the exact moment of film breakdown, the heat flux noted before a dry area was observed on the tube was taken as the breakdown heat flux $q_{w,B}$. In all cases the film breakdown was noted at the end of the heating length. The dry area moved upstream with increasing heat flux and caused, as expected, increasing wall temperatures.

Power loss to the surroundings was determined by calibration runs, in which no liquid was flowing inside the tube. The power required to maintain a given wall temperature is the power loss for that wall temperature. The heat loss was approximately 10 percent of the heat input to the liquid film. The net power input is the difference between the total input and the power loss.

Minimum Film Thickness

When the liquid flow rate within the unheated conducting glass tube was gradually reduced, a flow condition was reached at which complete wetting of the glass surface could not occur. The film thickness corresponding to this minimum flow rate and calculated by equation (1) is called the minimum film thickness ($h = h_{min}$ for $\Gamma = \Gamma_{min}$). That this condition of nonwetting of a surface will occur without the aid of thermocapillary effects is consistent with equation (C31). Equation (C31) gives a zero breakdown heat flux at the minimum film thickness. Another method of determining the minimum film thickness is by extrapolation. A plot was made of the breakdown heat flux $q_{w,B}$ against the initial film thickness h_0 and the curve extrapolated to zero heat flux (fig. 5). The zero heat-flux condition on the curve of breakdown heat flux against the initial film thickness should correspond to the minimum film thickness as demonstrated by equation (C31).

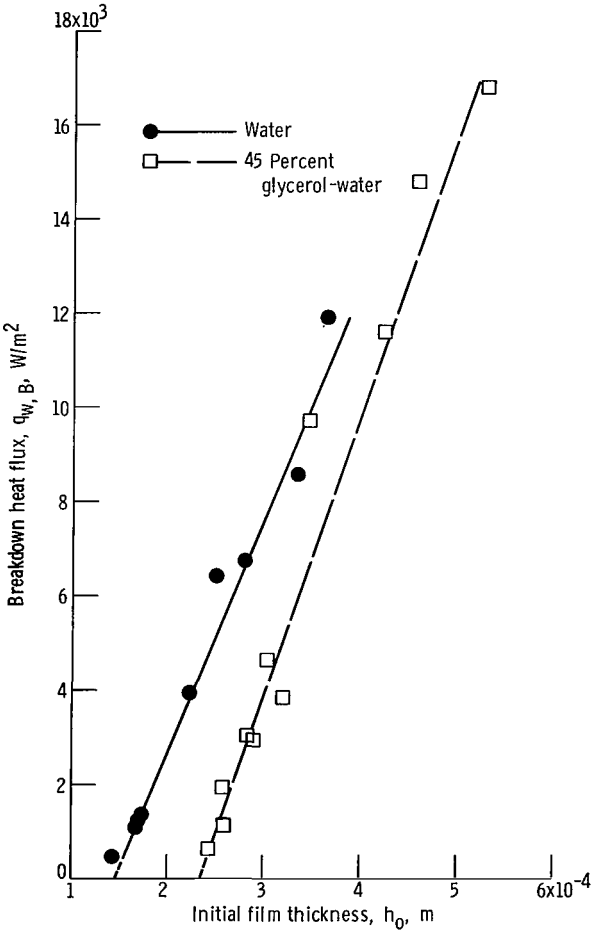

Figure 5. - Breakdown heat flux against initial film thickness. Heating length, 0.317 meter.

RESULTS AND DISCUSSION

Minimum Film Thickness

Table I shows the values of the minimum film thickness obtained by the two techniques described in the previous section. The film thickness values obtained by the two

TABLE I. - MINIMUM WETTING FILM THICKNESS

Fluid	Experimental	Extrapolation to zero, $q_{w,B}$	Reference 13
Water	1.4×10^{-4} m	1.47×10^{-4}	1.4×10^{-4}
45 percent glycerol-water	2.5	2.35	--------

methods agree with each other and are also in good agreement with the result obtained by Norman and McIntyre (ref. 13) for a copper pipe. Little information is presently available that could be utilized in the prediction of the minimum film thickness of a sheet of liquid which wets a cylindrical surface. A clue to the factors controlling the minimum film thickness may be found in an analysis for the minimum film thickness of a rivulet (ref. 20). This analysis, obtained by minimizing the surface and the kinetic energy, gives a minimum film thickness which is twice the value obtained in the present study. It appears, therefore, that while the analysis of reference 20 for a rivulet is not applicable herein, it is of value in showing direction for future study and in establishing the controlling quantity which is the Weber number. However, if we assume for a moment that the analysis of reference 20 is applicable to our system (based on an inspection of the equations) then it is of interest to attempt to explain the difference between the anlytical prediction of reference 20 of the minimum film thickness and the experimental value of this report. It is conceivable that as the liquid sheet thins down, it goes through a metastable condition that could result in film breakdown if sufficient disturbance energy were available. A liquid sheet in a metastable condition was observed by Griffith (ref. 21). Griffith noted that, if he gradually caused a horizontal liquid film to thin, the liquid film would remain in its original condition. Calculations made by Griffith indicated that, as the liquid film thinned down, it could no longer be stable in its original form, because of the increasing dominance of its surface force as compared with the body force. The fact that the liquid film would not change into a more stable configuration, as should be expected, makes the condition a metastable one.

While no analysis exists for the minimum film thickness as described herein, the analysis of reference 20 indicates the Weber number as the criterion for the minimum film thickness. Defining the Weber number as

$$We = \frac{\rho \overline{U}^2 h}{\sigma} \tag{3}$$

with

$$\overline{U} = \frac{\rho g h^2}{3\mu} \tag{4}$$

and using the experimental values of table I for calculations (extrapolated values), the Weber numbers for water and the glycerol-water solution (table II) are sufficiently close

TABLE II. - MINIMUM WETTING FILM THICKNESS WEBER NUMBER

Fluid	Weber number
Water	0.0142
45 percent glycerol-water	.0148

to each other to assume a constant Weber number criterion for the minimum film thickness. Taking an average of the Weber numbers for water and glycerol-water as 0.0145 gives, after a rearrangement of the Weber number, an equation for the minimum film thickness

$$h_{min} = 0.666\left(\frac{\sigma}{\rho}\right)^{1/5}\left(\frac{\mu}{\rho g}\right)^{2/5} \tag{5}$$

Since equation (5) was derived for a liquid film on a glass surface, it is not presently clear whether equation (5) is applicable to other surfaces. There is some indication, based on the author's experience, that increased surface roughness (to a limiting degree)

will permit a stable liquid film which is thinner than that predicted by equation (5). This can be explained by the increased interaction between the liquid and the solid surface when the solid surface is roughened. However, if the surface roughness is comparable to the film thickness, a rough surface might promote film breakdown.

Film Breakdown

In this section, the experimental data of film breakdown are compared with equation (C31). In equation (C31), the film thickness at the entrance of the heating length, ($h = h_0$), is calculated from equation (1) using the total flow rate, and the minimum thickness is calculated from equation (5). The resulting calculations as well as the basic experimental data taken with the heated glass tube are shown in table III. In table III, the bulk temperature was measured in the reservoir at the exit of the heating tube. This measurement is different from the local bulk corresponding to the local wall temperature due to two reasons:

(1) The exit bulk temperature should be warmer than the local bulk temperature because of additional heating in the balance of the length.

(2) The reservoir bulk temperature should be slightly lower than the exit bulk temperature becasue of cooling of the reservoir.

These two errors somewhat compensate each other. Therefore, the reported bulk temperature should be lower than the local true bulk temperature. Representative differences between the reported bulk temperature and the local bulk temperature are 5 and 8 K for water and glycerol-water, respectively. The possible error in the calculation of the film thickness ratio h_0/h_{min} is 4 percent for water and 8 percent for glycerol-water.

The property grouping in equation (C31) contains the density, thermal conductivity and the temperature coefficient of surface tension. With the exception of the temperature coefficient of surface tension for the glycerol-water solution, the property values are readily available from the literature. The temperature coefficient of surface tension for water, glycerol, and a 45-percent-glycerol - water solution were measured by the authors. The measurement technique is explained in appendix D.

According to equation (C31) a plot of the left side of equation (C31) against the logarithm of the film thickness ratio ($\ln h_0/h_{min}$) on semilog paper should result in a straight line passing through the origin. The experimental breakdown data for glycerol-water and for water is calculated as suggested by equation (C31) (table III) and is plotted in figure 6. The figure shows that the data can be plotted according to a semilogarithmic

TABLE III. - HEATED GLASS TUBE DATA AND CALCULATIONS

Flow rate, Γ_0, kg/(m)(sec)	Fluid temperature, T_B, K	Reynolds number, R_e, $4\Gamma/\mu$	Initial film thickness, h_0, m	Minimum film thickness, h_{min}, m	Film thickness ratio, h_0/h_{min}	Thermo-capilary initiation length x_0, m	Breakdown heat flux, $q_{w,B}$, W/m^2	$q_{w,B}(L - x_0)$, W/m	$q_{w,B}(L-x_0)\frac{\beta}{g}$	Inside wall temperature, K		
										$T_{w,1}$	$T_{w,2}$	$T_{w,3}$
45-percent glycerol-water; length, 0.317 m												
168×10^{-3}	302.2	195	5.28×10^{-4}	2.39×10^{-4}	2.21	0.007	168×10^2	5.20×10^3	4.13×10^{-5}	303	306	314
127	306.2	167	4.60	2.27	2.03	.0046	148	4.62	3.66	305	307	314
61.2	308.2	86.5	3.49	2.22	1.57	.002	97.2	3.06	2.43	305	308	311
28.7	302.2	33.3	2.91	2.39	1.22	.001	29.5	.932	.738	304	305	308
40.0	303.2	47.4	3.22	2.34	1.38	.0015	38.7	1.23	.972	---	---	---
20.7	303.2	24.5	2.58	2.34	1.10	.001	11.1	.351	.278	301	302	304
89.3	303.2	106	4.22	2.34	1.80	.0035	116	3.64	2.89	302	304	311
289	301.2	326	6.34	2.40	2.64	.011	150	4.59	3.64	302	304	315
33.6	303.2	39.8	3.04	2.34	1.30	.0012	46.8	1.48	1.17	300	303	307
19.2	300.2	20.7	2.59	2.42	1.07	.001	19.6	.619	.490	301	303	308
15.3	298.2	15.5	2.44	2.49	.980	.001	6.54	.206	.164	300	303	305
26.6	301.8	30.4	2.85	2.37	1.20	.001	30.1	.950	.754	301	303	306
47-percent glycerol-water; length, 0.317 m												
85.2×10^{-3}	300.7	85.6	4.39×10^{-4}	2.50×10^{-4}	1.76	0.004	162×10^2	5.08×10^3	4.02×10^{-5}	305	308	318
380	304.2	427	6.96	2.39	2.91	.014	161	4.88	3.86	307	309	325
455	309.2	611	6.96	2.22	3.14	.014	279	8.44	6.70	---	---	---
728	310.2	1010	8.06	2.20	3.66	.018	370	11.0	8.76	310	310	325
251	296.2	216	6.58	2.66	2.47	.012	170	5.18	4.11	300	301	317
194	299.2	184	5.90	2.54	2.32	.0095	174	5.36	4.26	303	303	317
382	301.2	390	7.19	2.48	2.90	.0145	233	7.05	5.60	304	304	316
318	305.2	373	6.48	2.36	2.75	.0118	159	4.85	3.85	302	302	312
47-percent glycerol-water; length, 0.164 m												
316×10^{-3}	306.2	383	6.38×10^{-4}	2.32×10^{-4}	2.75	0.0115	304×10^2	4.66×10^3	3.69×10^{-5}	305	306	---
238	306.2	288	5.79	2.32	2.50	.009	309	4.79	3.80	303	325	---
121	316.2	206	4.14	2.04	2.03	.0035	458	7.20	6.70	308	311	---
26.8	298.2	24.6	3.05	2.59	1.18	.00125	86.3	1.41	1.12	300	308	---
20.2	299.2	19.2	2.74	2.54	1.08	.001	32.2	.525	.417	309	311	---
45.8	309.2	61.1	3.25	2.25	1.44	.0016	184	2.98	2.36	306	311	---
47-percent glycerol-water; length, 0.0668 m												
28.4×10^{-3}	299.2	27.0	3.10×10^{-4}	2.54×10^{-4}	1.22	0.00135	236×10^2	1.55×10^3	1.23×10^{-5}	308	---	---
64.9	299.2	61.7	4.07	2.54	1.60	.0032	613	3.91	3.09	---	---	---
20.7	299.2	19.7	2.77	2.54	1.09	.0008	104	.687	.544	307	---	---
37.8	299.2	35.9	3.38	2.54	1.33	.0018	356	2.32	1.84	---	---	---
Water; length, 0.317 m												
20.2×10^{-3}	298.9	91.8	1.75×10^{-4}	1.47×10^{-4}	1.19	0.001	13.5×10^2	0.427×10^3	0.911×10^{-5}	302	303	305
18.9	299.1	86.3	1.71	1.47	1.16	.001	12.7	.405	.863	---	---	305
11.5	298.9	52.2	1.45	1.47	.986	.001	4.61	.146	.313	---	---	303
3.87	299.0	17.6	1.01	1.47	.687	.001	.915	.0289	.0617	---	---	301.9
194	301.2	928	3.64	1.44	2.53	.0095	119	3.66	7.82	---	---	306
65.5	303.2	327	2.51	1.42	1.77	.004	64.2	2.04	4.36	---	305	307
86.3	298.2	387	2.82	1.48	1.91	.0055	67.2	2.13	4.54	299	301	306
41.7	298.2	186	2.24	1.48	1.51	.003	39.6	1.25	2.67	300	301	303
16.5	296.8	71.4	1.66	1.50	1.11	.001	10.3	.326	0.696	301	302	304
151	301.7	730	3.35	1.44	2.33	.008	86.0	2.66	5.68	301	303	305
231	301.7	1120	3.84	1.44	2.67	.010	143	4.39	9.36	301	303	304
Water; length, 0.164 m												
8.48×10^{-3}	295.2	35.4	1.33×10^{-4}	1.52×10^{-4}	0.875	0.001	6.24×10^2	0.102×10^3	0.218×10^{-5}	302.0	302.6	---
13.1	295.2	54.7	1.57	1.52	1.03	.001	19.2	.313	.668	301	301	---
29.8	298.6	134	1.99	1.48	1.34	.002	38.5	.624	1.33	301	302	---
60.4	298.6	273	2.53	1.48	1.71	.004	90.4	1.44	3.08	300	306	---
93.8	298.2	420	3.00	1.48	2.03	.0065	102	1.61	3.43	294	305	---
124	298.2	555	3.20	1.48	2.16	.0075	112	1.76	3.76	301	308	---
214	304.2	1090	3.71	1.41	2.63	.0097	264	4.07	8.68	301	305	---
148	299.7	685	3.35	1.47	2.28	.0083	176	2.75	5.87	300	305	---
124	298.2	555	3.20	1.48	2.16	.0075	129	203	4.33	299	304	---

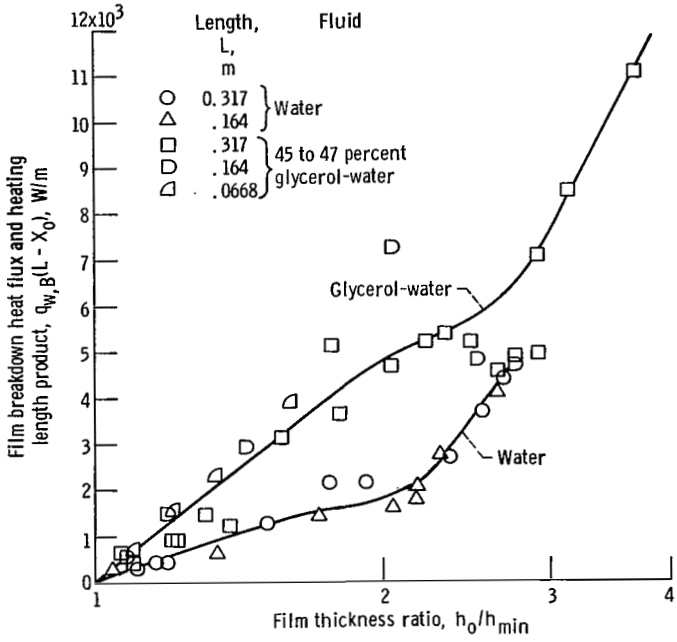

Figure 6. - Film breakdown heat flux and heating length product as function of film thickness ratio.

relation. In reference 1 the authors reported that the product of the breakdown heat flux and the heated length remained a constant value for a given flow condition. The plot of the experimental data shown in figure 6 tends to substantiate this conclusion of reference 1.

From figure 6 two regions can be discerned. They appear to correspond to two flow patterns of a falling film: the capillary-wave region for low flow rates, and the roll-wave region for higher flow rates. In between these two regions, there is a transition zone.

Capillary-wave region (region I). - In the capillary wave region, the wave amplitude is small and the presence of waves does not greatly alter the basic hydrodynamic model of breakdown. When breakdown of the film occurs, the surface remains dry and is not rewetted.

Plotting the film breakdown data with the physical-property grouping of equation (C31) (fig. 7) shows that the data points of water and glycerol-water solution merge into a single line originating at the origin ($h_0/h_{min} = 1$) and ending at the beginning ot the roll-wave region ($h_0/h_{min} = 2.1$). Thus, equation (C31) is applicable in the capillary-wave region (region I). The parameter b^2 can be determined from the slope of the line for the range of film-thickness ratio (h_0/h_{min}) between 1 and 2.1. The semi-analytical correlation thus obtained is

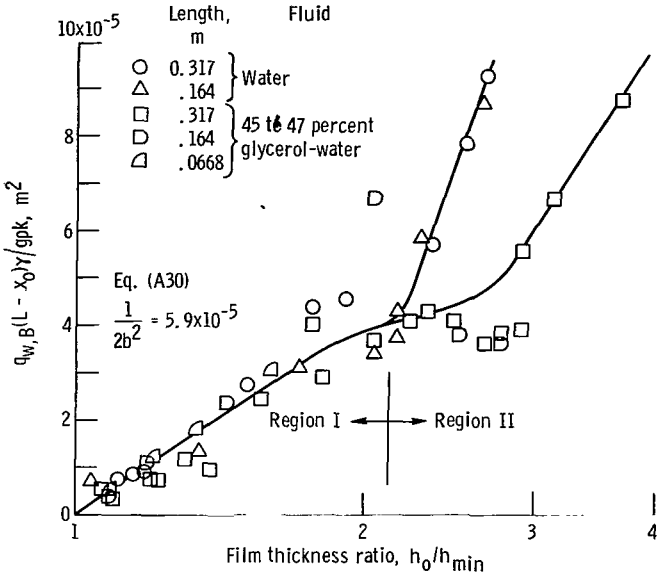

Figure 7. - Correlation of film breakdown heat flux according to equation (A30).

$$q_{w,B} = 5.9\times10^{-5}\,\frac{\rho k g}{(L - x_0)\,|\gamma|}\,\ln\frac{h_0}{h_{min}} \tag{6}$$

From equation (C25) it can be deduced that the derivation which leads to equation (6) is probably valid only when $bz < 1$; otherwise the profile of the film thickness would increase with z faster than physically possible. Therefore, the constant $1/b$ can be considered to be of the same order of magnitude as half of the wavelength existing on the liquid film, that is, $(\lambda/2)b < 1$. From the value of the coefficient of equation (12) the constant b can be calculated, since

$$\frac{1}{2b^2} = 5.9\times10^{-5}\ m^{-2}$$

Therefore, $b = 1$ reciprocal centimeter. The wavelength data for water of reference 1 ranged between 0.15 to 0.38 centimeter. This wavelength data and the calculated value of b satisfies the inequality of

$$\frac{\lambda b}{2} < 1$$

Thus it appears that the calculated value of b is consistent with the physical nature of the liquid film.

Roll-wave region (region II). - Figure 7 shows separate data plots for water and glycerol-water for a film thickness ratio greater than 2.1. A characteristic of this region is the presence of waves which appear to roll down independent of the liquid fluid. Once a dry area begins to form, it is rewetted by a roll wave causing the area to be alternately dry and wet. When sufficient heat is applied (breakdown heat flux), the dry area becomes stable. In this region, the slopes of the data plot in figure 7 are steeper than in region I. Apparently, the rewetting process is determined by the heat flux and temperatures at the S-L-V intersection, and a separate analytical treatment is required beyond the hydrodynamic model proposed in this paper. Figure 7 suggest that the transition condition from region I to region II as expressed by the film thickness ratio could be higher for glycerol-water. While this is possible, the authors have taken the position that the transition for glycerol-water is more gradual. On this basis, the film thickness ratio of 2.1 is taken as expressing the transition of water and glycerol-water from regions I to II. This position is also acceptable from an analytical point of view as is shown in the next section.

Transition between the two regions. - The transition from capillary-wave region to roll-wave region is signaled by the first appearance of alternative drying and rewetting of the heating surface. The authors studied this phenomenon (reported in ref. 1) and found that drying occurs at a wave valley and rewetting occurs when a wave crest passes over. Apparently, the wave crests in the capillary-wave region do not have sufficient momentum to overrun a dry area while the roll waves can. The momentum is required to overcome the surface force at the S-L-V intersection. Interestingly, the balance of inertial force against the surface force of liquid hanging over a dry spot is precisely the analytical model proposed by Hartley and Murgatroyd (ref. 20) which is applicable to the rewetting of a surface. Such a force balance results in the equation

$$h^* = 1.72\left[\frac{\sigma(1 - \cos\varphi)}{\rho}\right]^{1/5}\left(\frac{\mu}{\rho g}\right)^{2/5} \tag{7}$$

where h^* is the film thickness required to overrun the dry spot. Thus the criterion for the transition of capillary-wave region to roll-wave region is

$$h_p \geq h^* \tag{8}$$

where h_p is the film thickness of a wave crest. In reference 1 measurements were made of the peak film thickness that will rewet a surface. The results of these measurements were compared with equations (7) and (8). Agreement between the experiments

and equations (7) and (8) was possible if a contact angle of 90° was used. Although a 90° contact angle is greater than the static contact angle, it is probably consistent with wetting of a vertical surface. It is possible to conceive of an advancing vertical liquid film going through a range of contact angle prior to wetting of the surface. In this situation surface wetting would begin to occur after a 90° contact angle is reached and thus 90° can be considered as a critical contact angle. Use of equation (7) permits calculation of the peak film thickness that marks the transition between region I and region II. A relation between the peak thickness and the average thickness is needed. In reference 2 an analysis by Kapitsa for wavy film flow is presented. This analysis shows how the peak thickness and the average thickness are related in wavy flow.

$$h_p = h_0(1.21) \tag{9}$$

Taking the ratio of equation (7) to equation (5) and using equation (9), the analytical value of the transition film thickness ratio (h_0/h_{min}) is 2.1. It should be noted at this point that the ratio of equation (7) to equation (5) is a ratio of Weber numbers. The analytical value of the transition film thickness ratio compares very well with the experimental value shown in figure 7 of 2.1.

CONCLUSIONS

Observations of a heated falling liquid film gave some insight into the mechanism of film breakdown. It appears that a surface shear force created by a lateral surface tension gradient causes a gradual thinning of the liquid film as it flows over the heating surface. The film thins to a minimum thickness that is unstable and breaks down, leaving the heated surface exposed.

An analytical equation was derived based on visual results for the effect of thermocapillary instability on liquid film breakdown. It agreed with the experimental data up to a film thickness ratio h_0/h_{min} of 2.1. Beyond this ratio a separate plot for each fluid was required.

The experimental results indicate a change in the film breakdown mechanism for values of the film thickness ratio h_0/h_{min} greater than 2.1. The change in the manner in which film breakdown occurs appears to mark the transition from a capillary-wave region to a roll-wave region. The transition film thickness ratio can be predicted with the analysis of Hartley and Murgatroyd (ref. 20). The transition film thickness and the minimum film thickness that will wet a surface can be expressed in terms of a Weber number.

Experiment and analysis confirm the results of reference 1 that the product of the breakdown heat flux and the heated length $q_{w,B}L$ is a constant for given flow rate.

Lewis Research Center,
National Aeronautics and Space Administration,
Cleveland, Ohio, October 9, 1969,
120-01.

APPENDIX A

ESTIMATE OF INTERFACIAL VAPORIZATION

It is important to evaluate the role that vaporization plays in the present experiments. This is done in order to put on a better foundation our assumption that a surface-tension mechanism is the cause of film breakdown.

Neglecting convection within the falling liquid film and thus assuming heat transfer by conduction only, it is possible to write the heat balance as follows:

$$q_w = i\frac{d\Gamma}{dx} \tag{A1}$$

Equation (A1) expresses the decrease in the flow rate per unit length that results from vaporization at the interface. Integration of equation (A1) results in the following expression

$$q_w L = i(\Gamma_0 - \Gamma_f) \tag{A2}$$

To estimate the percent change of the initial flow rate Γ_0 equation (A2) is written

$$\frac{\Gamma_0 - \Gamma_f}{\Gamma_0} = \frac{q_w L}{\Gamma_0 i} \tag{A3}$$

For a representative calculation the largest heating length employed in the experiment and the highest heat flux and flow rate for the glycerol-water system (table III) are used

Wall heat flux, q_w, W/m^2	3.70×10^4
Heating length, m	0.317
Initial liquid flow rate, Γ_0, kg/(m)(sec)	0.713
Heat of vaporization, i, J/kg	2.41×10^6
Bulk temperature, K	310.2
Fractional change of initial flow rate, $(\Gamma_0 - \Gamma_f)/\Gamma_0$	0.0068

In terms of the initial film thickness, the change due to vaporization is as follows:

$$\frac{h_0 - h_f}{h_0} = 0.002$$

This calculation demonstrates that the role vaporization plays in the film breakdown mechanism is small enough to be neglected.

APPENDIX B

EFFECT OF VISCOSITY VARIATION ON FILM BREAKDOWN MECHANISM

A possible explanation for the gradual thinning of a liquid film that is being heated, is the decrease in fluid viscosity due to an increase in the temperature of the heated film as it flows down the vertical channel. An estimate of the temperature change to be expected, can be made by using a heat balance equation. The temperature change can then be related to viscosity change and a corresponding change in the film thickness. The heat balance is expressed as

$$q_w = \Gamma_0 c_p \frac{dT_B}{dx} \tag{B1}$$

or

$$T_{B,f} - T_{B,o} = \frac{q_w L}{\Gamma_0 c_p} \tag{B2}$$

Using the data of table III a representative calculation is made of the bulk temperature change due to heating.

$$T_{B,f} - T_{B,o} = 4.7 \text{ K} \tag{B3}$$

This temperature change is translated to the effect of the viscosity change on film thickness by the following equations:

$$h \sim \mu^{1/3} \tag{B4}$$

$$\frac{h_0}{h_f} = \left(\frac{\mu_0}{\mu_f}\right)^{1/3} \tag{B5}$$

Use of equations (B5) and (B3) and the initial bulk temperature presented in table III gives

$$\frac{h_0}{h_f} = 1.034 \tag{B6}$$

or

$$\frac{h_0 - h_f}{h_0} = 0.033 \tag{B7}$$

The viscosity effect appears to be an order of magnitude more significant than vaporization (appendix A) but can be classified along with vaporization as not being significant to the film breakdown mechanism.

APPENDIX C

DERIVATION OF EQUATIONS

What follows is an analysis of the liquid motion caused by lateral surface tension gradients which results in the liquid film being reduced to a minimum stable value condition ($h = h_{min}$). The analysis applies prior to, but not after, the physical breakdown of the film.

For simplicity, some assumptions are hypothesized for the model (fig. 3).

(1) The convective terms and inertia terms in the energy and momentum equations are negligible.

(2) One-dimensional steady-state heat conduction is assumed.

(3) The presence of waves on the interface would not affect the quasi-steady-state solution in both momentum and energy equations.

(4) Average film thickness is used even though waves are present in reality.

(5) The y-direction velocity is negligible.

(6) $\frac{\partial^2 U}{\partial x^2} << \frac{\partial^2 U}{\partial y^2}$ and $\frac{\partial^2 W}{\partial x^2} << \frac{\partial^2 W}{\partial y^2}$

(7) The wall heat flux is uniform.

(8) The surface tension force in the x-direction is small compared with the gravitational force.

Basic equations:

Momentum equation in x-direction

$$\rho g + \mu \frac{\partial^2 U}{\partial y^2} = 0 \tag{C1}$$

Momentum equation in z-direction

$$\mu \frac{\partial^2 W}{\partial y^2} = 0 \tag{C2}$$

Energy equation

$$k \frac{\partial^2 T}{\partial y^2} = 0 \tag{C3}$$

Continuity equation

$$\frac{\partial U}{\partial x} + \frac{\partial W}{\partial z} = 0 \tag{C4}$$

The integral form of the continuity equation (i. e., overall mass balance)

$$\frac{\partial \Gamma_x}{\partial x} + \frac{\partial \Gamma_z}{\partial z} = 0 \tag{C5}$$

where

$$\Gamma_x = \rho \int_0^h U \, dy \tag{C6}$$

$$\Gamma_z = \rho \int_0^h W \, dy \tag{C7}$$

Differentiating Γ_x and Γ_z, keeping in mind that h varies with x and z, results in

$$\frac{\partial \Gamma_x}{\partial x} = \rho \int_0^h \frac{\partial U}{\partial x} \, dy + \rho U(h) \frac{\partial h}{\partial x} - \cancel{\rho U(o, x)} = 0 \tag{C8}$$

$$\frac{\partial \Gamma_z}{\partial z} = \rho \int_0^h \frac{\partial W}{\partial z} \, dy + \rho W(h) \frac{\partial h}{\partial z} - \cancel{\rho W(o, x)} = 0 \tag{C9}$$

Combining equations (C8) and (C9) with (C5) and using equation (C4) yield

$$U(h) \frac{\partial h}{\partial x} + W(h) \frac{\partial h}{\partial z} = 0 \tag{C10}$$

Solutions:

Equation (C1) is the differential equation for the classical case of a falling film. The boundary conditions are

$$\left.\begin{aligned} U &= 0 \quad \text{at} \quad y = 0 \\ \frac{\partial U}{\partial y} &= 0 \quad \text{at} \quad y = h \end{aligned}\right\} \tag{C11}$$

The solution of equation (C1) subject to these boundary conditions is

$$U = \frac{g\rho}{\mu}\left(hy - \frac{y^2}{2}\right) \tag{C12}$$

Thus,

$$U(h) = \frac{g\rho}{\mu}\frac{h^2}{2} \tag{C12a}$$

For the flow in the z-direction, the boundary conditions are

$$W = 0 \quad \text{at} \quad y = 0 \tag{C13a}$$

$$\mu\frac{\partial W}{\partial y} = \frac{\partial \sigma}{\partial z} = \frac{d\sigma}{dT}\frac{\partial T}{\partial z}\bigg|_h \tag{C13b}$$

This equation is the balance of thermocapillary force against the viscous shear at the interface. The solution of equation (C2), satisfying boundary conditions of equation (C13) is

$$W = \frac{\gamma \left.\dfrac{\partial T}{\partial z}\right|_h y}{\mu} \tag{C14}$$

$$W(h) = \frac{\gamma \left.\dfrac{\partial T}{\partial z}\right|_h h}{\mu} \tag{C14a}$$

where

$$\gamma = \frac{d\sigma}{dT}$$

The boundary condition for the temperature equation is

$$\left.\begin{aligned} T &= T_w && \text{at } y = 0 \\ \left.\frac{\partial T}{\partial y}\right|_w &= -\frac{q_w}{k} && \text{at } y = 0 \end{aligned}\right\} \tag{C15}$$

Solutions of equation (C3), satisfying equation (C15) are

$$k\frac{\partial T}{\partial y} = k\left.\frac{\partial T}{\partial y}\right|_w = -q_w \tag{C16}$$

$$T = T_w - \frac{q_w}{k}y \tag{C17}$$

Thus at $y = h$

$$T(h) = T_w - \frac{q_w}{k}h \tag{C18}$$

Differentiating equation (C18) with respect to z, with the assumption that T_w is a weak function of z, and combining with equation (C14a) yields

$$W(h) = -\frac{q_w \gamma}{k\mu}\frac{\partial h}{\partial z}h \tag{C19}$$

Eliminating $W(h)$ and $U(h)$ from equation (C10) by using equation (C12a) and (C19) results in

$$\frac{g\rho}{\mu}\frac{h^2}{2}\frac{\partial h}{\partial x} - \frac{q_w \gamma}{k\mu}\left(\frac{\partial h}{\partial z}\right)^2 h = 0$$

or

$$\left(\frac{\partial h}{\partial z}\right)^2 = Ah\frac{\partial h}{\partial x} \tag{C20}$$

where

$$A = \frac{g\rho k}{2\gamma q_w} \tag{C21}$$

Using the separation of variable technique call

$$h = aX(x)Z(z) \tag{C22}$$

The solution for Z is

$$\frac{Z'}{Z} = \pm b \quad \text{or} \quad Z = c_1 \exp \pm bz$$

Since the film thickness should be increasing with the distance from z = 0, we should have

$$\left.\begin{aligned} Z &= c_1 \exp bz \qquad \text{for } z > 0 \\ Z &= c_1 \exp -bz \qquad \text{for } z < 0 \end{aligned}\right\} \tag{C23}$$

The solution for X is

$$X = c_2 \exp \frac{b^2 x}{A} \tag{C24}$$

An expression of equation (C22) in terms of equations (C23) and (C24) is

$$h = c_3 \exp |bz| \exp \frac{b^2 x}{A} \tag{C25}$$

The free surface of the film will not begin to experience lateral motion with respect to the main flow until the thermal layer grows to the size of the film thickness. Therefore, the film thickness will remain unchanged for a small initial length ($x_0 \approx 1$ cm). This condition is expressed as follows

$$h = h_0 \qquad \text{for } x \leq x_0 \tag{C26}$$

Where the initial length x_0 was derived in reference 1 and is given by

$$x_0 = \frac{\mu}{\sqrt{hg\rho}} U_h^+ \int_0^{h^+} U^+ dy^+ - \int_0^{h^+} (U^+)^2 dy^+ \tag{C27}$$

At any given position we have

$$h = h \quad \text{at} \quad x = x \tag{C28}$$

Therefore, with conditions (C26) and (C28) equation (C25) may be written

$$\frac{h}{h_0} = \exp \frac{b^2(x - x_0)}{A} = \exp\left[\frac{2\gamma q_w b^2 (x - x_0)}{g\rho k}\right] \tag{C29}$$

Note that γ is negative, thus h diminishes with increasing x. When $h = h_{min}$ the film is unstable and about ready to break up. This will first occur at the end of the heating length or at $x = L$. At $x = L$ equation (C29) becomes

$$\frac{h_{min}}{h_0} = \exp\left[\frac{2\gamma q_{w,B} b^2 (L - x_0)}{g\rho k}\right] \tag{C30}$$

or

$$q_{w,B} = \frac{g\rho k}{(L - x_0) 2\gamma b^2} \ln \frac{h_{min}}{h_0} \tag{C31}$$

APPENDIX D

TEMPERATURE COEFFICIENT OF SURFACE TENSION

Measured temperature coefficients of surface tension exist for water and glycerol, but values of the coefficient for a mixture of water and glycerol are not, to our knowledge, available. Therefore, it was necessary to experimentally determine the temperature coefficient of surface tension of a 45-percent-by-weight glycerol-water solution. The change of the surface tension as a function of temperature was determined from the measurement of the surface pull on a circular platinum ring. The force exerted on the ring by the liquid surface is related to the surface tension as follows:

$$\sigma = \frac{Ff_c}{2c} \tag{D1}$$

where f_c is a correction factor determined by Harkins and Jordan (ref. 22). By varying the temperature of the fluid, the temperature coefficient of surface tension was calculated using equation (D1)

$$\gamma = \frac{\Delta\sigma}{\Delta T} = \frac{\Delta(Ff_c)}{\Delta\ T2c} \tag{D2}$$

Before beginning the surface tension measurements, the platinum ring was cleaned and flamed. At any given temperature, which was kept constant by a constant temperature bath, the force exerted on the ring by the liquid surface was measured with very sensitive electronic balance. A small percentage of the voltage output from the electronic balance was picked up with an x-y recorder. By plotting a small percentage of the output from the electronic balance, it was possible to make accurate as well as rapid measurements of surface tension changes with temperature. The two axes of the x-y recorder permitted a record of force against time. The force against time record is important because of the force difference between the maximum surface pull and the force when the ring breaks the surface. The surface tension is calculated from the maximum pull.

The results obtained for the temperature coefficient of surface tension are shown in table IV. The value of the temperature coefficient of surface tension for water and glycerol were obtained without much difficulty and were in good agreement with the literature values. The initial surface-tension determinations for the glycerol-water solution were erratic. This behavior could be avoided by submerging the platinum ring below

TABLE IV. - TEMPERATURE COEFFICIENT

OF SURFACE TENSION

Fluid	This report	Reference 25
Water	1.3×10^{-4} N/m$^{\circ}$R	1.5
Glycerol	.60	.598
45-percent glycerol - 55-percent	.38	-----

the surface of the liquid and waiting approximately 3 minutes before making a surface-tension measurement. It is conceivable that this technique permitted the surface molecules to attain their equilibrium states. In this situation, where the surface has been allowed to age, the surface tension has the static value as opposed to a dynamic value for a fresh surface. Since a dynamic surface tension is a function of time, it would be difficult to reproduce. This would account for the initial erratic results when a surface-tension measurement was made immediately after the platinum ring broke the liquid surface as it was immersed in the liquid. It is interesting to note that the temperature coefficient of surface tension for glycerol-water is lower than either water or glycerol alone. This apparent anomaly was also noted for mixtures of ethyl alcohol and water and for methyl alcohol and water by Valentiner and Hohls (ref. 23).

Hansen (ref. 24) reports temperature dependent deviations from a mean value of the temperature coefficient of surface tension for water. He interprets these deviations as signifying the complexity of the water interface. That such a result might be applicable to glycerol-water solutions is not known. The present experiments assure a temperature coefficient of surface tension independent of temperature, as is commonly accepted.

REFERENCES

1. Hsu, Y. Y.; Simon, F. F.; and Lad, J. F.: Destruction of a Thin Liquid Film Flowing Over a Heating Surface. Chem. Eng. Progr. Symp. Ser., vol. 61, no. 57, 1965, pp. 139-152.

2. Levich, Veniamin G.: Physicochemical Hydrodynamics. Prentice-Hall, Inc., 1962, pp. 384, 684.

3. Yih, Chia-Shun: Fluid Motion Induced by Surface-Tension Variation. Phys. Fluids, vol. 11, no. 3, Mar. 1968, pp. 477-480.

4. Mitchell, W. T.; and Quinn, J. A.: Convection Induced by Surface Tension Gradients: Experiments with a Heated Point Source. Chem. Eng. Sci., vol. 23, no. 5, June 1968, pp. 503-507.

5. Yih, Chia-Shun: Instability of Laminar Flows due to a Film of Adsorption. J. Fluid Mech., vol. 28, pt. 3, May 26, 1967, pp. 493-500.

6. Ludviksson, V.; and Lightfoot, E. N.: Hydrodynamic Stability of Marangoni Films. AIChE. J., vol. 14, no. 4, July 1968, pp. 620-626.

7. Pearson, J. R. A.: On Convection Cells Induced by Surface Tension. J. Fluid Mech., vol. 4, pt. 5, Sept. 1958, pp. 489-500.

8. Nield, D. A.: Surface Tension and Bouyancy Effects in Cellular Convection. J. Fluid Mech., vol. 19, pt. 3, July 1964, pp. 341-352.

9. Scriven, L. E.; and Sternling, C. V.: On Cellular Convection Driven by Surface - Tension Gradients: Effects of Mean Surface Tension and Surface Viscosity. J. Fluid Mech., vol. 19, pt. 3, July 1964, pp. 321-340.

10. Scanlon, J. W.; and Segel, L. A.: Finite Amplitude Cellular Convection Induced by Surface Tension. J. Fluid Mech., vol. 30, pt. 1, Oct. 17, 1967, pp. 149-162.

11. Block, Myron J.: Surface Tension as the Cause of Bénard Cells and Surface Deformation in a Liquid Film. Nature, vol. 178, 1956, pp. 650-651.

12. Norman, W. S.; and Binns, D. T.: The Effect of Surface Tension Changes on the Minimum Wetting Rates in a Wetted-Rod Distillation Column. Trans. Inst. Chem. Engrs. (London), vol. 38, no. 6, 1960, pp. 294-300.

13. Norman, W. S.; and McIntyre, V.: Heat Transfer to a Liquid Film on a Vertical Surface. Tran. Inst. Chem. Engrs. (London), vol. 38, no. 6, 1960, pp. 301-307.

14. Hallett, V. A.: Surface Phenomena Causing Breakdown of Falling Liquids Films During Heat Transfer. Int. J. Heat Mass Transfer, vol. 9, no. 4, Apr. 1966, pp. 283-294.

15. Shibuya, I.: Rept. Inst. High Speed Mech., Tohoku Univ. 1, 17, (1951).

16. Yih, Chia-Shun: Stability of Parallel Laminar Flow with a Free Surface. Proceedings of the Second U. S. National Congress of Applied Mechanics. Paul M. Naghdi, ed., ASME, 1955, pp. 623-628.

17. Kapitza, P. L.: Undular Flow of Thin Layers of a Viscous Fluid. I. Free Flow. Zhur. Eksptl. Teoret. Fiz., vol. 18, Jan. 1948, pp. 3-18.

18. Benjamin, T. Brooks: Wave Formation in Laminar Flow Down an Inclined Plane. J. Fluid Mech., vol. 2, pt. 6, Aug. 1957, pp. 554-574.

19. Nusselt, Wilhelm: Der Wärmeaustausch am Berieselungskühler. Zeit. Ver. deut. Ing., vol. 67, no. 9, Mar. 3, 1923, pp. 206-210.

20. Hartley, D. E.; and Murgatroyd, W.: Criteria for the Break-up of Thin Liquid Layers Flowing Isothermally over Solid Surfaces. Int. J. Heat Mass Transfer, vol. 7, Sept. 1964, pp. 1003-1015.

21. Griffith, P.; Lee, K. S.; Chung, K. R.; and Hunt, B. L.: Three Problems in Capillarity. Dept. Mech. Eng., Massachusetts Inst. Tech., circa 1962.

22. Harkins, William D.; and Jordan, Hubert F.: A Method for the Determination of Surface and Interfacial Tension from the Maximum Pull on a Ring. J. Am. Chem. Soc., vol. 52, no. 5, May 1930, pp. 1751-1772.

23. Valentiner, S.; and Hohls, H. W.: Oberflächenspannungen von Alkohol-Wasser-Mischungen. Zeit. B. Physik, vol. 108, no. 1/2, Dec. 20, 1937, pp. 101-106.

24. Drost-Hansen, Walter: Aqueous Interfaces. Methods of Study and Structural Properties. Part II. Chemistry and Physics of Interfaces. Am. Chem. Soc., 1965, pp. 22-41.

25. Partington, James R.: The Properties of Liquids. Vol. 2 of An Advanced Treatise on Physical Chemistry. Longmans, Green and Co., 1951, p. 194.

NATIONAL AERONAUTICS AND SPACE ADMINISTRATION
WASHINGTON, D. C. 20546

OFFICIAL BUSINESS

FIRST CLASS MAIL

POSTAGE AND FEES PAID
NATIONAL AERONAUTICS AND
SPACE ADMINISTRATION

"The aeronautical and space activities of the United States shall be conducted so as to contribute . . . to the expansion of human knowledge of phenomena in the atmosphere and space. The Administration shall provide for the widest practicable and appropriate dissemination of information concerning its activities and the results thereof."

—NATIONAL AERONAUTICS AND SPACE ACT OF 1958

NASA SCIENTIFIC AND TECHNICAL PUBLICATIONS

TECHNICAL REPORTS: Scientific and technical information considered important, complete, and a lasting contribution to existing knowledge.

TECHNICAL NOTES: Information less broad in scope but nevertheless of importance as a contribution to existing knowledge.

TECHNICAL MEMORANDUMS: Information receiving limited distribution because of preliminary data, security classification, or other reasons.

CONTRACTOR REPORTS: Scientific and technical information generated under a NASA contract or grant and considered an important contribution to existing knowledge.

TECHNICAL TRANSLATIONS: Information published in a foreign language considered to merit NASA distribution in English.

SPECIAL PUBLICATIONS: Information derived from or of value to NASA activities. Publications include conference proceedings, monographs, data compilations, handbooks, sourcebooks, and special bibliographies.

TECHNOLOGY UTILIZATION PUBLICATIONS: Information on technology used by NASA that may be of particular interest in commercial and other non-aerospace applications. Publications include Tech Briefs, Technology Utilization Reports and Notes, and Technology Surveys.

Details on the availability of these publications may be obtained from:

SCIENTIFIC AND TECHNICAL INFORMATION DIVISION

NATIONAL AERONAUTICS AND SPACE ADMINISTRATION

Washington, D.C. 20546